SEMI-EMPIRICAL ESTIMATION OF SIGNIFICANT WAVE HEIGHT USING SENTINEL-1 SAR : *HOW IS IT DIFFERENT IN OFF-SHORE AND COASTAL WATERS?*

Fabian Surya Pramudya,[1,3], Jiayi Pan[1,2], and Adam T. Devlin[2]
[1]Institute of Space and Earth Information System, The Chinese University of Hong Kong
Email: fabian.surya@link.cuhk.edu.hk, panj@cuhk.edu.hk
[2]School of Marine Sciences, Nanjing University of Information Science and Technology, Nanjing, Jiangsu, China
Email: adam_devlin@cuhk.edu.hk
[3]Centre for Remote Sensing, Institute of Technology, Bandung (CRS-ITB), Indonesia.

KEYWORDS: Significant Wave Height, Sentinel-1 SAR, Semi-empirical Estimation.

ABSTRACT: In the last four decades, quantitative measurements of significant wave height (SWH) by the use synthetic aperture radar (SAR) radar cross section (RCS) has been proven effective in different approaches, even without prior knowledge of wind information. Using a recent system of Sentinel-1 SAR, this paper will propose a semi-empirical update of an existing simple semi-empirical algorithm for simple narrow-band swell-wave spectrum that developed in 1982, to quantify the dependency of SWH in coastal and offshore waters, in different sea states. We also propose a preliminary empirical method for determining the backscatter cross-section to incidence angle function for vertical polarization in a 5.405 GHz SAR system, aided by adaptive filtering of RCS and least square estimation of parameters used in the algorithm. Adaptive filtering and least square estimated parameters ensures a statistically robust determination of the backscatter cross-section to incidence angle function and dominant wave length identification, as clearer wave patterns can be revealed by higher image contrast level. Standard meteorological buoy data from National Buoy Data Center (NDBC) is used in development of the empirical model through validation. This research employs Level-1 GRD Sentinel-1A and 1B SAR images from 2016 to early 2017 in 7 NDBC station, with more than 90 valid measurement points in Hawaii and the central part of the west coast of the United States of America. Those are selected to represent deep to shallow water depth and river influenced estuaries. However, extreme sea states are not considered due to the limitation of the developed algorithm, image repository, and buoy data availability. Beside the two analysis methods described above, additional detailed analyses are conducted on the sea state relation to the velocity bunching mechanism, based on SWH estimation result.

1. INTRODUCTION

Nowadays, SAR systems are widely available covering many resolutions, but very few of them are open to public. C-Band (5.405 GHz) Sentinel-1A and 1B are among the systems that could be publicly accessed, offering a reliable and continuous observation for monitoring the ocean surface. Over the past 40 years, the potential of using digitally processed and corrected synthetic aperture radar (SAR) image spectra of the ocean surface has been quantitatively proven for being able to measure many wave parameters such wavelength, wave direction, wave slope, and wave height of the ocean wave (Valenzuela, 1978, Alpers, 1981), in order to explain phenomena such as significant wave height, internal wave, and swell and wind induced wave (Alpers, 1985, Chapron, 2001, Marghany, 2002, Hersbach 2007, Shao 2016).

Wave height is one of the most important characteristics of ocean wave that plays an important role for harbor and coastal engineering (Jinsong, 2004), and significant wave height becomes the value that represent the most prominent information of wave height over time. As the importance of significant wave height for supporting anthropogenic activities becomes higher in coastal areas, especially in the region which relying on many coastal activities, increasing the need of continuous monitoring. To implement that application, it is necessary to have a clear picture of the physical processes involved in the electromagnetic ocean-surface interaction, and a reasonably accurate analytical description of the processes must be available in order to extract the desired ocean variables (Valenzuela, 1978).

Most of the wave parameter estimation of the SAR two-dimensional image spectrum, including significant wave height, requires the wave occurrence to be imaged. Although the image is not directly related to any actual two-dimensional height-variance spectrum of the actual wave parameters (Alpers, 1981; Beal, 1983). This complicated process resulted an urge of theoretical and empirical understanding of the SAR sensor limitation under specific sea surface environment trough dependency analysis to paramters known involved. (Valenzuela, 1978 Alpers 1981, Vesecky and Stewart, 1982, Beal, 1983).

Dependency analysis on the open ocean has been recently done by Grieco (2017) using the Sentinel-1A SAR system specifically for estimating significant wave height in the low to medium sea state environment with several parameters, such as wind speed and wavelength cut-off. The result shows that the dependency of the wavelength cut-off on the square root of

the significant wave height is approximately linear while the dependency on the wind speed is approximately linear only if the sea state is fully developed, which on the most cases, the wave pattern is visible on the SAR image.

The result in Shao (2016) shows that the reliability of using the VV-polarization of the Sentinel-1 SAR images with 81.7% accuracy of wave height validated using National Buoy Data Center (NDBC) floating buoy. In general, recent result shows that semi-empirical estimation of ocean wave parameters, aided by dependency analysis could lead to an empirical one-to-one dependency of parameter-to-parameter model, determination of constants value, and more suitable geophysical transfer function, while overcoming the need of wind input or other first-guessed parameters.

This preliminary study will emphasize on updating a classic methods of significant wave height estimation based on (Beal, 1983) and Valenzuela (1978) in coastal and offshore area, with tuned for the Sentinel-1A and IB dataset. Although those studies have stated it's own limitation of the non-extreme sea state condition and range travelling waves, due to the dominant, a detailed dependency analysis could establish a meaningful empirical understanding the surface wave imaged by Sentinel-1 SAR represented in deep to shallow water depth and river influenced estuaries, and investigate the capability of Sentinel-1 SAR system in imaging various ocean surface phenomenon.

2. METHODOLOGY

Thomas (1982) developed a transfer function for narrow-band swell-wave spectrum to estimate Hs, based on the Valenzuela (1978) empirical model of root mean square slope of the sea surface. Mentioned in Thomas (1982), due to the linear function used, this transfer function is limited into for waves propagating in a direction which is approximately perpendicular to the flight direction, doppler shift effects (or known as *velocity bunching*) smaller, leaving the effect of lifting and tilting of the Bragg scattering waves by the long-wavelength gravity waves that create a modulation in the image (known as *tilt modulation*) (Wright et al. 1980, Alpers, 1981). Although, it is known that in most of the cases this classic method is resulting overestimated significant wave height over measurement data. Where f is the mean sea surface, significant wave height of Hs is given by:

$$Hs = 4\sqrt{f(r,t)^2} \tag{1}$$

Basic transfer function accommodating a narrow-band swell-wave spectrum centered on wavenumber K_o, wavelength of λo, and root mean square slope of the sea surface $tan\theta$ is denoted by

$$\frac{tan\theta}{Hs} = \frac{|K_o|}{4} = \frac{\pi}{2\lambda o} \tag{2}$$

Improving the estimated result, linear fitting were applied to estimate more robust variable weight value of $\boldsymbol{a}$ and $\boldsymbol{b}$ using 29 image, as follow

$$Hs = \frac{\boldsymbol{a}\, 2\lambda o\, .\boldsymbol{b}\, tan\theta}{\pi} \tag{3}$$

Where estimated value of a and b are 0.85 and respectively. Updating the Valenzuela (1978) empirical model of root mean square slope of the sea surface, five equally distanced transects divided from the first to the last row of the entire column of the part of the image that classified as water body. Transects are taken along the range direction to ensure the maximum range of scan and accommodate any effects that may occurs during the data acquisition by imitating the scanning procedure. More detailed workflow procedures are following flowchart shown in Figure 1 below.

3. DATASETS

This research employs 93 valid measurement points of Level-1 GRD Sentinel-1A and 1B VV-polarization SAR from 2016 to early 2017 while 7 NDBC measurement buoys are used in parameter estimation, validation, and dependency analysis. 29 Images are used as sampled image for constant approximation trough linear fitting, and others are used as validation and analysis purposes. Figure 2 below shows the footprint of Sentinel-1 with the location of the measurement buoys in Hawaii and the central part of the west coast of the United States of America. Those are selected to represent deep to shallow water depth and river influenced estuaries.

Figure 3 shows more detailed information about data and parameter distribution. The number of coastal area data used are much fewer than the off-shore due to the availability of wave crest imaged by the SAR sensor.

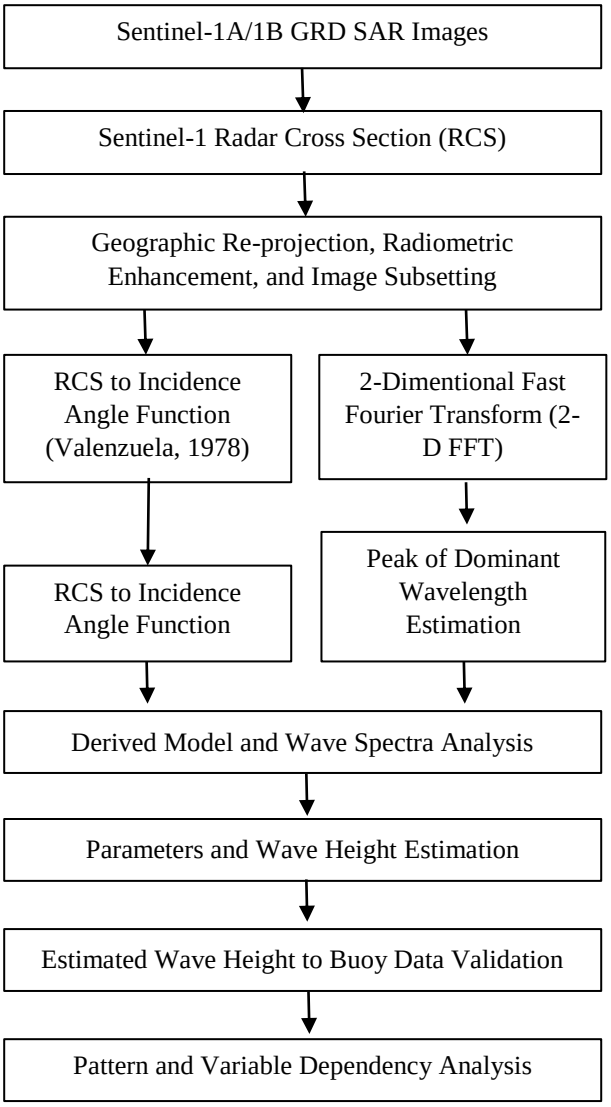

Figure 1. Research workflow

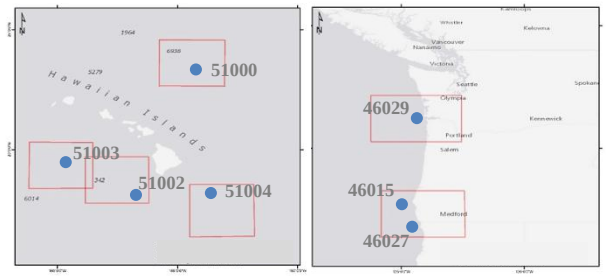

Figure 2. Map of Sentinel-1 scene footprints and co-located NDBC measurement buoy position (Source: ESRI, GEBCO, NOAA, and other contributors)

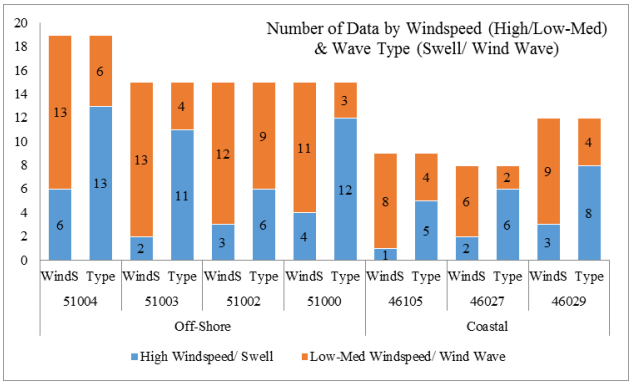

Figure 3. NDBC Buoys and Sentinel-1 data distribution based on parameters: Classified wind speed and wave type

4. RESULT AND ANALYSIS

Figure 4 and Figure 5 below shows the overall result of the significant wave height estimation and it's dependency on several circumstances or parameters Statistical comparison of significant wave height above shows both usability of the linear semi-empirical equation used and may explain and improve our understanding how Sentinel-1 system visually respond in imaging wave in off-shore and coastal location, trough many sea condition, which are mainly influenced by wind, such as wind speed and wave type.

We found it is hard to analyze both separately since the Sentinel-1 RCS are used as the main input for the algorithm, hence directly affecting the estimated significant wave height. Figure xx (a) trough (c) shows the general idea of the wave crest linearity imaged in both locations, the off-shore and coastal on the left and right side, respectively followed on the other subfigure in both Figure xx and Figure xx. Generally, the off-shore SWH result shows higher linear fit to the NDBC buoys, with one of the highest R2 value of 0.629 and 0.44 m RMSE when all data gathered, and not significantly change in low-to-high wind speed and wind wave condition. Higher R2 value of 0.807 and 0.37 m of RMSE are noticed in the swell dominated ocean surface. On the contrary, the coastal water plots are not showing the same satisfying result, with lower correlation

coefficient and higher RMSE. The best statistical result is also found in the swell dominated ocean surface, with R2 and RMSE value of 0.807 and 0.37 m respectively.

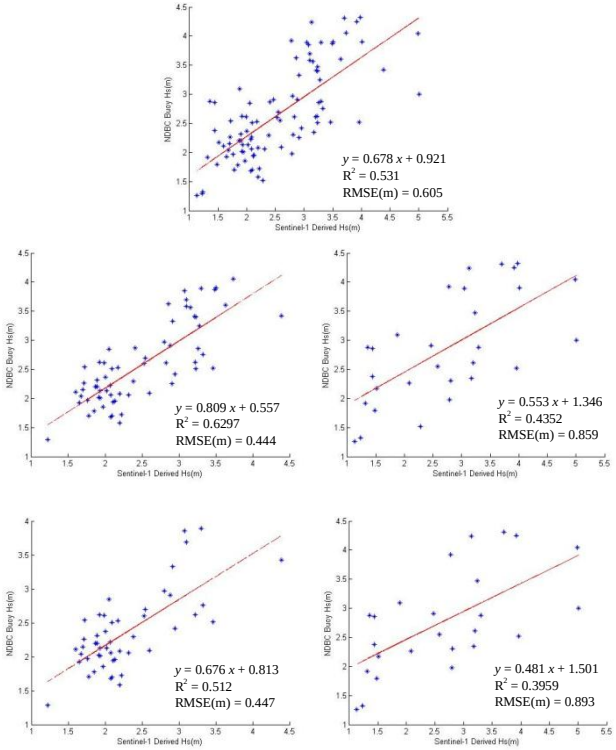

Figure 4. Comparison of retrieved significant wave height from Sentinel-1 in VV polarization and 7 *in situ* NDBC buoy from November 2016 – April 2017 in all available data (a), in off-shore location (b), and in coastal area (c), with 10m above sea surface wind speed under 10 m/s in off-shore location (d), and in coastal area (e).

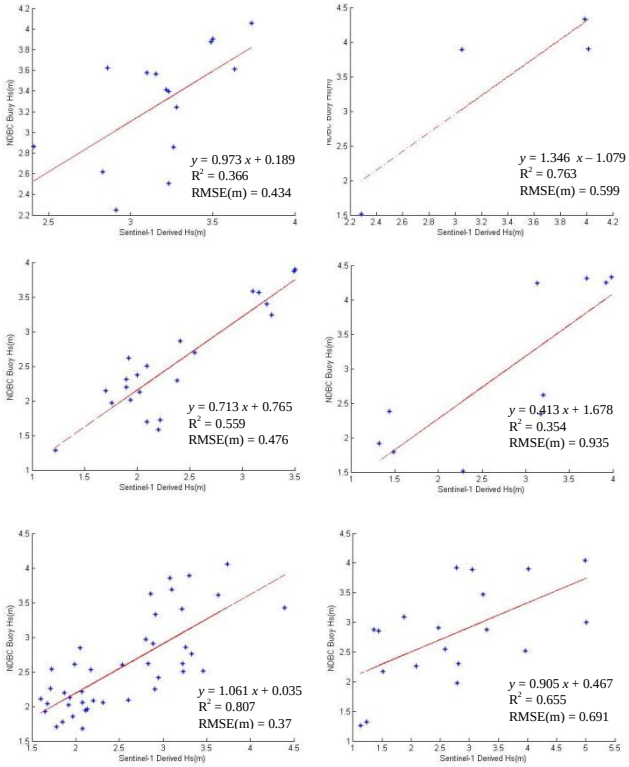

Figure 5. Comparison of retrieved significant wave height from Sentinel-1 in VV polarization and 7 *in situ* NDBC buoy from November 2016 – April 2017 in all available data (a), in off-shore location (b), and in coastal area (c), with 10m above sea surface wind speed under 10 m/s in off-shore location (d), and in coastal area (e).

Figure 6 below compares randomly chosen RCS, 2-dimentional wave spectra, and radar cross-section to incidence angle function of off-shore (*upper*) and coastal area (*lower*), used as additional qualitative analysis of statistical result retrieved before. The upper left and center sub-figures show clearly visible and linearly patterned wave crest imaged by the Sentinel-1. Having an 180^{o} ambiguity, the dominant wave direction could be visually recognized as north-easterly or south-westerly wave. As the 2D-FFT were applied to the RCS, the directional wave spectra shows only one pair of symmetrical peak between 200 – 100m wavelength with approximately the same direction of the dominant wavelength.

The lower left RCS is also showing a visible but more distanced wave crest, or longer wavelength, with also linear but less clear pattern in the coastal area, with qualitatively estimated from the crest lines, the waves are abiguitively moving toward north-south direction. But, a closer look to the zoomed image will show us another east-west wave with shorter wavelength, as seen in the directional wave spectra with the multiple dominant pairs of symmetrical peak, one between 200 – 100m wavelength and others more than 200m. In determining the dominant wavelength in most of the coastal area's cases, the peak with the highest amplitude will not always be the wavelength that we want as the input for the algorithm. It is the secondary wavelength ranged from 75-125m that resulting the best fit of SWH to the NDBC buoys.

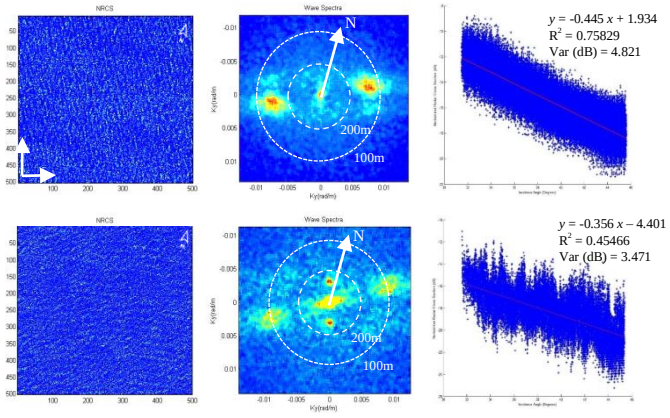

Figure 6. Comparisons of retrieved 2-D Sentinel-1 Radar Cross Section (*a*), wave spectra (*b*), and Sentinel-1 RCS to incidence angle plot (*c*) in off-shore location, and in coastal area (*d*), (*e*), (*f*).

Both phenomena understood from the examples are also reflected in the radar cross-section to incidence angle function graph of the sampled transects. The side-looking platform will resulting a general pattern of backscattering power that is always decreasing along the increasing incidence angle, due to the increasing range from the platform to the target. In the most cases of the off-shore waters, the statistics shows higher fit to the linear regression with the higher variance of backscattering power.

On the coastal waters, however, the function graph showing much lower correlation coefficient value of R2 to the linear regression, and variance value, but higher mean backscattering power, due to more wave crests imaged. Visually, the multiple dominant wavelength are also shown by the less smooth pattern compare to the upper graph, indicating much more capillary wave crest and non-linear features appeared on the sea surface of coastal area.

5. CONCLUSION

Comparing all the result, constant distribution of plotted points, R^2, and RMSE value show that linear approximation is statistically sufficient to accommodate general condition of significant wave height in off-shore areas, while widely sparse points in coastal location gives general ideas on how linear approximation is not yet sufficient to accommodate coastal areas general due to multiple dominant wavelength occurrences.

Overall result reflect the basic empirical characteristics on how Sentinel-1 imaged the water surface response to approximately the same wind forcing on the ocean surface in off-shore and coastal area. [1] Wave type are classified based on the difference of the surface wind direction and mean wave direction measure by the buoys. More than 45^o difference between those two parameters, we consider the occurring wave as a swell. Swell and wind wave occurrences are hardly found to be related with any specific wind input parameters in our datasets. Figure xx shows some buoys on off-shore waters could also be dominated by wind waves and vice versa. [2] The σw/Iw, Var(dB), and Tan(θr) are parameters derived according to Valenzuela (1978) seen in Figure 4 and Figure 5, showing bigger variance of off-shore waters. Higher variance values are resulted by the range of contrast from the wave crest with the higher backscattering power to the lower crest trough or flat surface, while the surface characteristic of coastal waters are dominated by visually non-linear capillary waves with ranges of frequencies, resulting smaller range of backscattering coefficient with less darker part of the image. Calculated from transect along the range direction, the variance are found not being affected by the number of transect pixels chosen. [3] The dominant wavelength in the coastal area is found to be shorter than in the off-shore water, ranged approximately from 90-125m. In several cases, when more than two dominant wavelengths are appeared within the range and close to each other, the wind input direction and mean wave direction information from the NDBC buoys could be useful to determine the desired dominant wavelength. [4] In most of the cases, the estimated significant wave height are over-estimated, compared to the NDBC buoys, but the errors are usually bigger in the coastal area due to the non-linear effect that affecting the dominant wavelength determination and decreased the variation of the RCS value along the incidence angle

6. REFERENCES

[1] Alpers,W. R., and Hasselmann, K..1978. The Two-Frequency Microwave Technique For Measuring Ocean-Wave Spectra From an Airplane or Satellite, *Boundary Layer Meteorol*.,13, 213-230.

[2] Alpers,W. R., and Rufenach, C. L.. 1979. The Effect of Orbital Motions on Synthetic Aperture Radar Imagery of Ocean Waves, *IEEE Trans. Antennas Propag*., AP-27, 685-690.

[3] Alpers,W. R., Ross, D.B., and Rufenach, C.L..1981. On The Detectability of Ocean Surface Waves by Real and Synthetic Aperture Radar, *J. Geophys.Res,*, 86, 6481-6498.

[4] Beal, R. C., Tilley, D. G., and Monaldo, F. M.. 1983. Large and Small Scale Spatial Evolution of Digitally Processed Ocean Wave Spectra from Seasat Synthetic Aperture Radar, *J. Geophys. Res.*, 88,1761-1778.

[5] Grieco, G., Nirchio, F., Migliaccio, M., Portabella, M.. 2016. Dependency of The Sentinel-1 Azimuth Wavelength Cut-Off on Significant Wave Height and Wind Speed. *Int. J. Remote Sensing*, ISSN : 1366-59013

[6] Shao,W.Z., Zhang, Z., Li, X., and Li, H.. 2016. Ocean Wave Parameters Retrieval from Sentinel-1 SAR Imagery. *Remote Sens*. doi:10.3390/rs8090707.

[7] Thomas, M.H.B..1982. The Estimation of Wave Height From Digitally Processed SAR Imgaery. *Int. J. Remote Sensing*, 3, 63-68

[8] Valenzuela, G.R. 1978. Theories for The Interaction of Electromagnetic and Oceanic Waves—A Review. *Bound-Lay Meteorol.13*, 61–85.

[9] Vachon, P.W.; Krogstad, H.E.; Paterson, J.S. 1994. Airborne And Spaceborne Synthetic Aperture Radar Observations of Ocean Waves. *Atmos. Ocean*. *32*, 83–112.

[10] Vesecky, J.F.,and R.H.Stewart, The Observation of Ocean Surface Phenomena Using Imagery from The Seasat Synthetic Aperture Radar: An Assessment, *J. Geophys. Res*.,87,3397-3430, 1982

[11] Wright, J. W., Plant, J. W., Keller, W. C., and Jones, W. L., 1980, *J. geophys. Res., 85*,4957Chapron, B.; Johnsen, H., and Garello, R.. 2001. Wave and Wind Retrieval from SAR Images of The Ocean. *Ann. Telecommun. 56*, 682–699.